Applied Catalysis B: Environmental 86 (2009) 98–107

Contents lists available at ScienceDirect

Applied Catalysis B: Environmental

journal homepage: www.elsevier.com/locate/apcatb

Photocatalytic reductive–oxidative degradation of Acid Orange 7 by polyoxometalates

A. Troupis, T.M. Triantis, E. Gkika, A. Hiskia *, E. Papaconstantinou *

Institute of Physical Chemistry, NCSR Demokritos, 153 10 Athens, Greece

ARTICLE INFO

Article history:
Received 13 May 2008
Received in revised form 30 July 2008
Accepted 1 August 2008
Available online 8 August 2008

Keywords:
Photocatalysis
Polyoxometalates
Azo dye
Acid Orange 7
Titanium dioxide

ABSTRACT

A series of polyoxometalates (POM) $PW_{12}O_{40}^{3-}$, $SiW_{12}O_{40}^{4-}$, $P_2W_{18}O_{62}^{6-}$ and $P_2Mo_{18}O_{62}^{6-}$ have been used as photocatalysts for the destruction of the azo dye Acid Orange 7 (AO). There are two ways to consider: reductive and oxidative decomposition. The reductive decomposition involves absorption of light by polyoxometalates, oxidation of an organic substrate, for instance propan-2-ol as sacrificial reducing reagent and reoxidation-recycling of the reduced polyoxometalates by the azo dye via a thermal (dark) reaction. AO is reduced to aromatic amine derivatives in a multi-electron process, as suggested by the analysis of the detected products and the obtained stoichiometry of the electron transfer process, following a first-order dependence for AO. This process takes place within a few minutes. On the other hand, photooxidative decomposition involves again absorption of light by POM followed by direct or OH-mediated oxidation of the dye. This process is an order of magnitude slower than reductive elimination, but leads to mineralization of AO. Several intermediates have been detected prior to evolution of CO_2.

The nature of the POM catalyst is decisive in the efficiency of reductive AO decoloration, following the order $PW_{12}O_{40}^{3-} > SiW_{12}O_{40}^{4-} > P_2W_{18}O_{62}^{6-} > P_2Mo_{18}O_{62}^{6-}$, that is their photooxidizing ability, in one-pot photolysis experiments. On the other hand the efficiency of thermal (dark) reaction between reduced POM and AO follows the reductive ability of POM, i.e., $SiW_{12}O_{40}^{5-} > PW_{12}O_{40}^{4-} > P_2W_{18}O_{62}^{7-} > P_2Mo_{18}O_{62}^{8-}$. The presence of electron scavengers suppresses the reductive degradation rate according to the trend $Ag^+ > O_2 > Cu^{2+} > Ni^{2+}$, while increase of pH retards decoloration.

Contrary to TiO_2, sensitized photodecomposition, i.e., absorption of light by AO and electron injection to POM has not been observed.

1. Introduction

The wide spread of dye industry, which amounts to more than 1 million tons annually, combined with the potential carcinogenic risk that these dyes as well as their degradation products cause severe environmental pollution. As more than half of the used dyes are azo dyes, extensively applicable in textiles, papers, leathers, gasoline, additives, food and cosmetics [1], it is essential to develop methods that can lead to destruction of such compounds. The traditionally used methods for azo dyes decoloration include adsorption on activated carbon or biological processes. Especially in the case of azo dyes, an interesting alternative solution involves the implementation of reductive process. As these dyes are easily reduced via cleavage of the azo-bond, electrolytic [2], chemical (using various reducing reagents such as sulfide [3] or metal iron [4] among others) or even natural reduction under anaerobic conditions, can lead to efficient dye decoloration. This foresees in a sequential process where biologically recalcitrant azo dyes are subjected firstly to reductive treatment and subsequently get amenable to biological or chemical oxidations [5].

1.1. TiO_2 and POM photocatalysis in reductive destruction of azo dyes

Advanced oxidation processes are well known for their oxidizing efficiency even in traces of the target compounds. Among these processes, TiO_2 and POM photocatalysis exhibit the further advantage of triggering combined oxidations/reductions in one-pot system. The reductive destruction of azo dyes by using the photochemically obtained TiO_2 (e) as reducing reagent has been exhibited by Kamat et al. [6–8]. In this case TiO_2 catalyst absorbs light and the excited state causes oxidation of the organic substrate, i.e., alcohols. The reducing species left in the solution

* Corresponding author. Tel.: +30 210 650 3642; fax: +30 210 6511766.
E-mail address: epapac@chem.demokritos.gr (E. Papaconstantinou).

0926-3373/$ – see front matter © 2008 Elsevier B.V. All rights reserved.
doi:10.1016/j.apcatb.2008.08.001

(photogenerated electrons on TiO_2) can reduce and decolorize the azo dyes.

Polyoxometalate anions (POM) include a large variety of oxygen-bridged metal clusters well known for their rich photocatalytic action [9,10], analogous to this of semiconductors [11]. POM are, relatively, not toxic and inexpensive. Their excited state, produced after absorption of UV–near vis light, is a strong oxidant able to mineralize, either directly or via OH radicals-mediated oxidations, plethora of organic species, including organic pollutants [12,13]. The photoreduced POM species can deliver the electrons to a great variety of chemical species, i.e., O_2 [14], H^+ [15], nitroaromatics [16] or metal ions [17–20]. Arslan-Alaton and Ferry had the inspiration to use $SiW_{12}O_{40}^{4-}$ as photocatalyst for the reductive destruction of AO [21,22], showing that the photochemically obtained 1 equiv. reduced 12-tungstosilicate, $SiW_{12}O_{40}^{5-}$, can efficiently reduce the AO dye with a rate constant of $5.2 \times 10^4\ M^{-1}\ s^{-1}$ [21]. Such a high rate is reasonable considering the feasibility that POM exhibit in a great variety of electron transfer reactions [23]. However, in these papers the action of solely $SiW_{12}O_{40}^{4-}$ was studied on AO decoloration, while no products of the anaerobic reductive degradation of the AO dye were mentioned [21].

Following our previous paper on Naphthol blue [24], herein we advance this notion, screening four polyoxometalate anions ($PW_{12}O_{40}^{3-}$, $SiW_{12}O_{40}^{4-}$, $P_2W_{18}O_{62}^{6-}$ and $P_2Mo_{18}O_{62}^{6-}$) of precisely and widely ranged redox properties (Scheme 1) in order to examine the influence of the kind of POM on the efficiency of the process. The effects of concentration of catalyst, propan-2-ol, dye or oxygen, as well as the influence of pH or the presence of metal ions such as nickel, copper and silver on the decoloration rate are investigated. The degradation products obtained during this photocatalytic process are also reported. Although the process is highly efficient in decolorizing aqueous solutions of the dye, a deeper insight is essential concerning the mineralization of the solution, as toxic amines (sulfanilic acid) are liberated upon AO reduction. Thus we have further studied, to a limited extend, the photooxidative decomposition of AO by POM. This process although much slower than the corresponding reductive elimination of AO, leads to mineralization of the dye. Several intermediates detected prior to mineralization are reported.

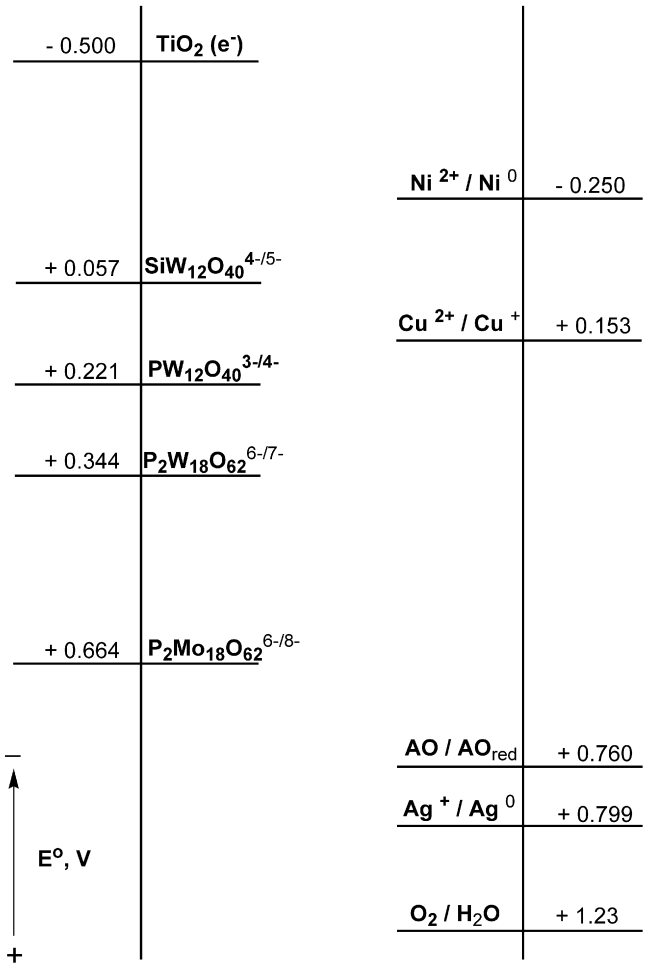

Scheme 1. Reduction potentials of the species involved (V vs. NHE).

2. Experimental

2.1. Materials and reagents

$H_4SiW_{12}O_{40}$ and $H_3PW_{12}O_{40}$ were purchased from Aldrich and PanReac, respectively, while $K_6P_2W_{18}O_{62}$ and $(NH_4)_6P_2Mo_{18}O_{62}$ were prepared according to literature methods [25,26]. $SiW_{12}O_{40}^{4-}$ and $P_2W_{18}O_{62}^{6-}$ are stable up to pH ca. 5.5, whereas $PW_{12}O_{40}^{3-}$ is stable at pH ca. 1 and $P_2Mo_{18}\ O_{62}^{6-}$ up to 2.5. However, since $PW_{12}O_{40}^{3-}$ is the most efficient in the degradation of the dyes, it is studied in more details in our experiments.

Acid Orange 7 was obtained from Aldrich with purity greater than 85%. Ultra pure water was obtained from a compact apparatus from Barnstead. $HClO_4$ was from Riedel de Haen and $NaClO_4$ was purchased from Aldrich (99+%). Extra pure argon (99.999%) and dioxygen (>99.95%) were used for deaeration or oxygenation of solutions.

2.2. Irradiation procedures

Illumination was performed with an Oriel 1000 W Xe arc lamp equipped with a cool water circulating filter to absorb the near IR radiation and a 320 nm cut-off filter in order to avoid direct photolysis of propan-2-ol. The incident radiation was reduced to about 40% with a slit diaphragm in order to obtain reasonable photolysis times. The total photonic flux (320–345 nm) determined by ferrioxalate actinometry was ca. 7.9×10^{-6} einstein min^{-1}.

Illumination was also performed with a laboratory constructed "illumination box" equipped with four F15W/T8 black light tubes (Sylvania GTE, USA). The maximum emission of these tubes is around 375 nm, emitting 71.7 $\mu W\ cm^{-2}$ at a distance of 25 cm.

For the reductive elimination of AO a typical experiment was as follows: 4 ml of aqueous dye solution containing propan-2-ol and POM catalyst was added to a spectrophotometer cell (1 cm path length), deaerated (or non-deaerated) and covered with a serum cap. The cell was mounted on a thermostated cell holder, under constant stirring, and the lamp focused with a lens on the contents. The temperature was $18 \pm 1\ ^\circ C$. The pH was adjusted at 1 with $HClO_4$ and the ionic strength was adjusted at 0.1 M, whenever necessary, with $NaClO_4$. Analysis was performed using all 4 ml of the photolyzed solution every time.

To have adequate quantities for the identification of intermediates by GC–MS, samples of 30 ml of the aqueous dye solution (1 mM) containing POM catalyst ($PW_{12}O_{40}^{3-}$, 10 mM) were added to a cylindrical pyrex cell (1 cm path length), oxygenated for 30 min, covered with a serum cap and photolyzed with the Oriel 1000 W Xe lamp.

The CO_2 formation was followed by headspace gas chromatographic analysis of the gas phase by GC–MS. A 4 ml solution was

placed in a 15 ml pyrex cell, oxygenated and photolyzed in the "illumination box".

2.3. Analytical procedures

The concentration of reduced POM in photolyzed deaerated or non-deaerated solutions was calculated from the known molar absorption coefficients of the 1 equiv. reduced 12-tungstophosphate, $PW_{12}O_{40}^{4-}$ (ε_{752} = 2000 M^{-1} cm^{-1}), 1 equiv. reduced 12-tungstosilicate, $SiW_{12}O_{40}^{5-}$ (ε_{730} = 2100 M^{-1} cm^{-1}), 1 equiv. reduced 18-tungstodiphosphate, $P_2W_{18}O_{62}^{7-}$ (ε_{909} = 4400 M^{-1} cm^{-1}) and 2 equiv. reduced 18-molybdodiphosphate, $P_2Mo_{18}O_{62}^{8-}$ (ε_{758} = 11,000 M^{-1} cm^{-1}) [27], using a Perkin Elmer Lambda 19 Spectrometer. The concentration of the dye molecules was measured from the known molar absorption coefficient of the Acid Orange 7 (ε_{484} = 20,587 M^{-1} cm^{-1}) [21].

The initial rate of dye degradation was measured from the slope of the curve obtained by monitoring the concentration of the dye in the photolyzed solutions vs. time, for the first ca. 30% of dye decoloration using a least squares treatment. At this stage, the error from intermediates absorbing at 484 nm must be minor.

The products of dye degradation were determined by HPLC. HPLC analysis was carried out using an HPLC apparatus consisted of a Waters (Milford, MA, USA) Model 600E pump associated with a Waters Model 600 gradient controller, a Rheodyne (Cotati, CA, USA) Model 7725i sample injector equipped with 20 μl sample loop, a reversed phase (RP) C_{18} analytical column by Phase sep (25 cm × 4.6 mm i.d., 5 μm) and a Waters Model 486 tunable absorbance detector controlled by the Millenium (Waters) software. Sulfanilic acid, the product of AO reduction, was monitored at 254 nm with a mobile phase consisting of water for 7 min and then methanol 20% for the next 10 min (flow rate 0.5 ml/min).

When the GC–MS was used for the identification of the intermediate products in the oxidative decomposition of AO, the photolyzed solution (30 ml) was extracted with dichloromethane (3× 20 ml). The organic layers were combined, dried over sodium sulfate, and then concentrated in a rotary evaporator to 1 ml.

GC–MS analysis was performed using an Agilent 6890 Series gas chromatograph interfaced to an Agilent 5973 mass selective detector (Wilmington, DE, USA). Data acquisition, processing, and instrument control were performed by the Agilent MSD Chem-Station software. The analytical column was an HP-5MS ((5%-phenyl)-methylpolysiloxane) capillary column, 30 m × 0.25 mm i.d., 0.25 μm film thickness. A split–splitless injector was used in splitless mode. The injector temperature was 250 °C and the injection volume 2.0 μl. Helium was used as a carrier gas at a flow rate of 1.0 ml/min. The oven temperature program was 50 °C for 4 min, 5 °C/min to 150 °C for 1 min, 5 °C/min to 280 °C for 10 min and the transfer line temperature 280 °C. Identification of the GC/MS spectral features was achieved with the use of a Wiley library. All library-matched species exhibited the degree of match better than 90%.

For the CO_2 analysis, 100 μl are sampled from the headspace of the photolyzed solution and injected into the GC/MS. Oven temperature is 40 °C and retained for 10 min after injection. Then there is a gradual increase in temperature at 5 °C/min up to 50 °C and finally temperature increase rate at 20 °C/min up to 80 °C, where it stops for 1 min. Extracted chromatograms on ion 44 were used for the detection and quantification of the CO_2.

3. Results

3.1. Photocatalytic reductive decoloration of AO

A deaerated solution (4 ml) containing AO 0.05 mM, propan-2-ol 0.5 M and the POM ($PW_{12}O_{40}^{3-}$) 0.25 mM was irradiated with UV–near vis light, λ > 320 nm, to examine the mechanism of the photocatalytic reduction and decoloration of the dye. Upon photolysis the decoloration of the AO solution takes place within a few minutes (Fig. 1), as derived from the lowering of the characteristic absorbance of AO at 484 nm. Prolonged illumination, after the AO has been completely destroyed, leads to the formation of the 1 equiv. reduced POM ($PW_{12}O_{40}^{4-}$ with characteristic absorbance at 752 nm) (Fig. 1).

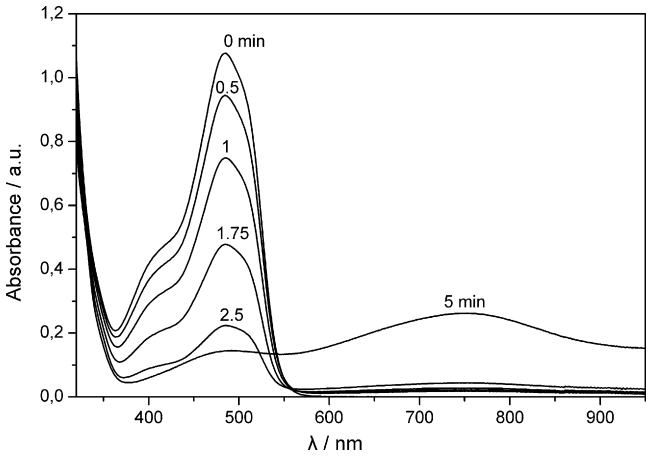

Fig. 1. Reductive decomposition: UV–vis spectra of photolyzed deaerated aqueous solutions containing propan-2-ol 0.5 M, $H_3PW_{12}O_{40}$ 0.25 mM, AO 0.05 mM at pH 1, for various irradiation times, showing the decoloration of AO as well the formation of the 1 equiv. reduced tungstate, $PW_{12}O_{40}^{4-}$ after 5 min of photolysis.

Sulfanilic acid is the main degradation product of AO degradation as a fraction of the azo-bond brake, according to HPLC measurements (Fig. 2). In this case, lower concentration of POM, 0.025 mM, and higher concentration of dye, 0.1 mM, are used in order to facilitate the analysis of degradation products.

3.1.1. Effect of POM

The influence of different POM photocatalysts on the initial rate of dye decoloration was investigated, keeping all the other experimental conditions constant (POM 0.25 mM, AO 0.05 mM, propan-2-ol 0.5 M, pH 1). Illumination of a deaerated solution containing propan-2-ol/POM/AO led to gradual decoloration, with a rate depending on the nature of POM catalyst. The efficiency of the process decreased in the order $PW_{12}O_{40}^{3-} > SiW_{12}O_{40}^{4-} > P_2W_{18}O_{62}^{6-} \gg$ no POM (Fig. 3).

In another series of experiments, deaerated POM 0.25 mM/propan-2-ol 0.5 M (pH 1) solutions, i.e., in the absence of dye, were

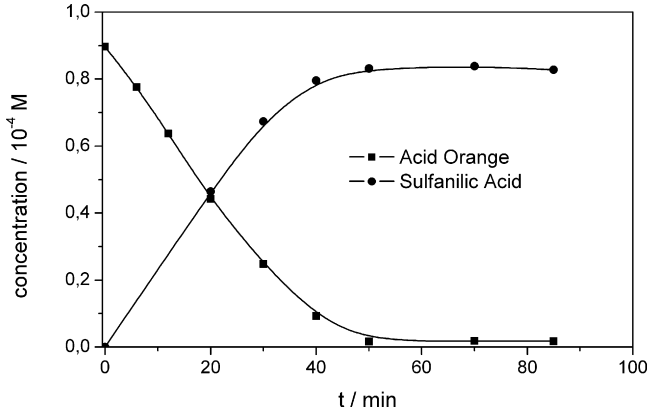

Fig. 2. Reductive decomposition: destruction of AO and concomitant formation of sulfanilic acid upon photolysis of a deaerated aqueous solution containing propan-2-ol 0.5 M, $H_3PW_{12}O_{40}$ 0.025 mM, AO 0.1 mM (pH 1).

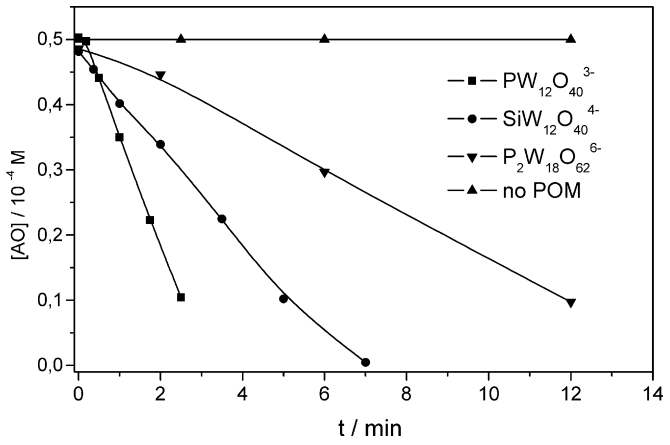

Fig. 3. Reductive decomposition: influence of POM photocatalyst, $PW_{12}O_{40}^{3-}$, $SiW_{12}O_{40}^{4-}$ and $P_2W_{18}O_{62}^{6-}$, on the rate of AO degradation upon photolysis of deaerated aqueous solutions containing propan-2-ol 0.5 M, POM 0.25 mM, AO 0.05 mM (pH 1).

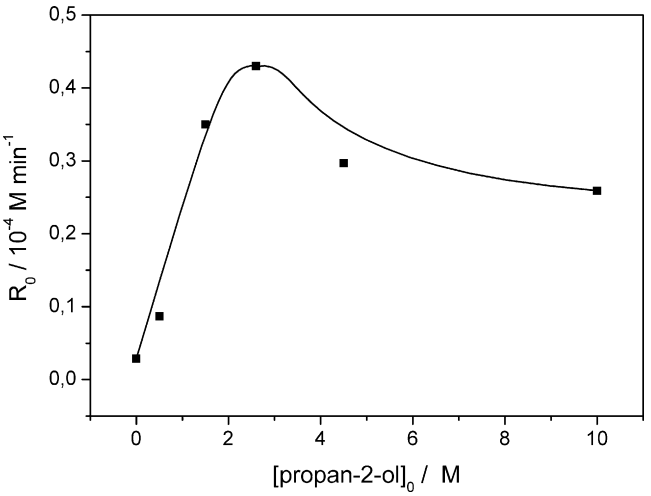

Fig. 5. Reductive decomposition: influence of propan-2-ol concentration on the initial rate, R_0, of AO decoloration. Non-deaerated solutions of $PW_{12}O_{40}^{3-}$ 0.25 mM, AO 0.05 mM (pH 1).

illuminated and the photochemical production of the one-electron reduced POM was monitored by its characteristic absorbance at ca. 750 nm at the initial stage of the photolysis. The rate of formation of the 1 equiv. reduced POM followed the above order, too. More specifically, the corresponding values for the photochemical formation of $PW_{12}O_{40}^{4-}$, $SiW_{12}O_{40}^{5-}$ and $P_2W_{18}O_{62}^{7-}$ were 1.2, 0.27 and 0.22 $\times$ 10^{-4} M min^{-1}, respectively.

3.1.2. Effect of POM concentration

Fig. 4 exhibits the influence of catalyst ($PW_{12}O_{40}^{3-}$) concentration on the initial rate of dye decoloration in non-deaerated solutions (AO 0.05 mM, propan-2-ol 0.5 M, pH 1). For concentrations of $PW_{12}O_{40}^{3-}$ below ca. 0.25 mM the initial rate of dye decoloration seems to increase proportionally (as is always the case) with the POM concentration, while for concentrations of $PW_{12}O_{40}^{3-}$ greater than ca. 1 mM the system reaches, practically, saturation in photon absorption and the rate becomes zero order with respect to the catalyst.

3.1.3. Effect of propan-2-ol concentration

Fig. 5 illustrates the variation of the initial rate of photocatalytic dye decoloration with the concentration of the propan-2-ol, in non-deaerated solutions ($PW_{12}O_{40}^{3-}$ 0.25 mM, AO 0.05 mM, pH 1). Again, linear dependence on propan-2-ol concentrations below ca. 1.5 M is observed reaching roughly saturation at larger concentrations.

3.1.4. Effect of AO concentration

The initial rate of dye destruction is also a function of the initial concentration of the dye (Fig. 6) (POM 0.25 mM, propan-2-ol 0.5 M, pH 1). This rate exhibits an optimum dye concentration (0.050 mM) above which further increase in the concentration value leads to decrease of the decoloration rate.

3.1.5. Effect of metal ions and oxygen

A solution of propan-2-ol 0.5 M, $PW_{12}O_{40}^{3-}$ 0.25 mM, AO 0.05 mM (at pH 1) oxygenated or deaerated containing also $NiSO_4$, $CuSO_4$ or $AgNO_3$ 1.2 mM, were photolyzed in order to examine the role of O_2, Ni^{2+}, Cu^{2+} or Ag^+, respectively in the efficiency of the photocatalytic process. As depicted in Fig. 7, the presence of Ni^{2+} ions does not affect the rate of AO decoloration while the efficiency of the process is influenced in the order $Cu^{2+} < O_2 < Ag^+$.

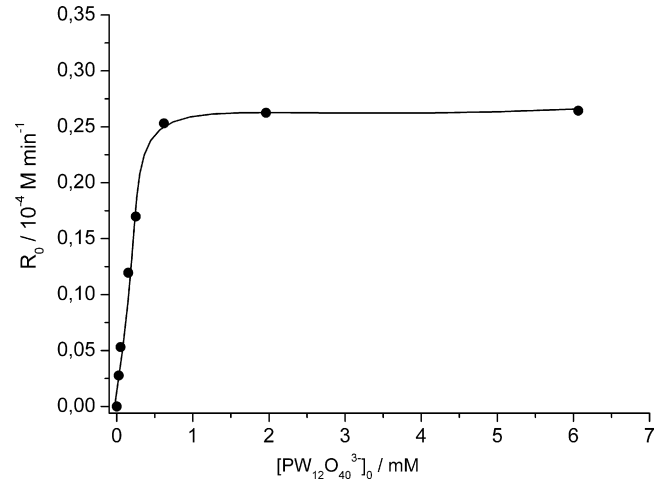

Fig. 4. Reductive decomposition: influence of $PW_{12}O_{40}^{3-}$ concentration on the initial rate, R_0, of AO decoloration. Non-deaerated solutions, propan-2-ol 0.5 M, AO 0.05 mM (pH 1).

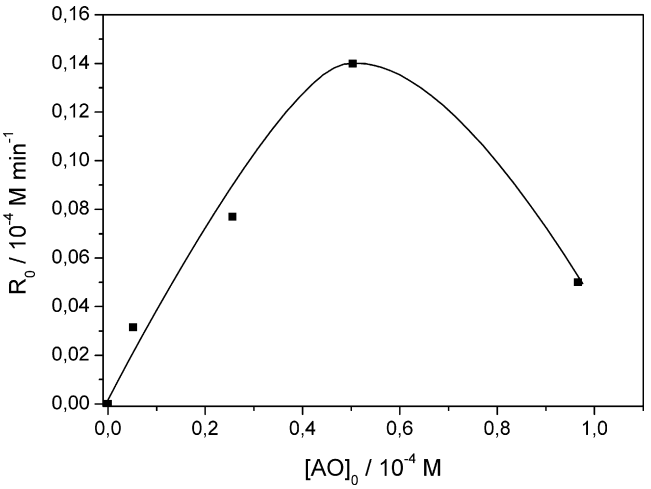

Fig. 6. Reductive decomposition: effect of AO concentration on the initial rate, R_0, of AO decoloration. Non-deaerated solutions of $PW_{12}O_{40}^{3-}$ 0.25 mM, propan-2-ol 0.5 M (pH 1).

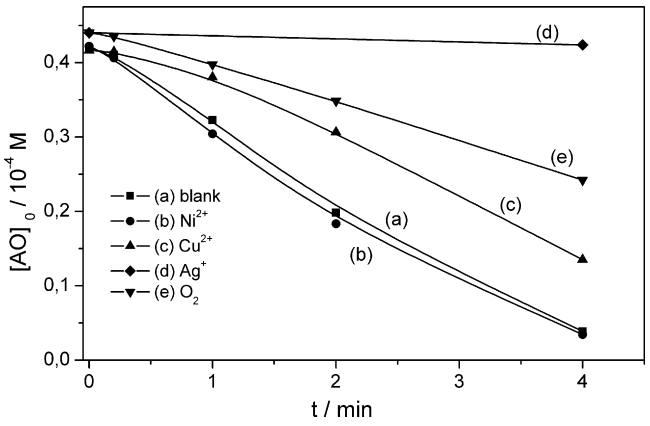

Fig. 7. Reductive decomposition: lowering of AO concentration in deaerated photolyzed solutions of propan-2-ol 0.5 M, $PW_{12}O_{40}^{3-}$ 0.25 mM, AO 0.05 mM (pH 1) in the absence (a) or in the presence of Ni^{2+} (b), Cu^{2+} (c), Ag^{+} (d). The data for an oxygenated photolyzed solution are also reported (e).

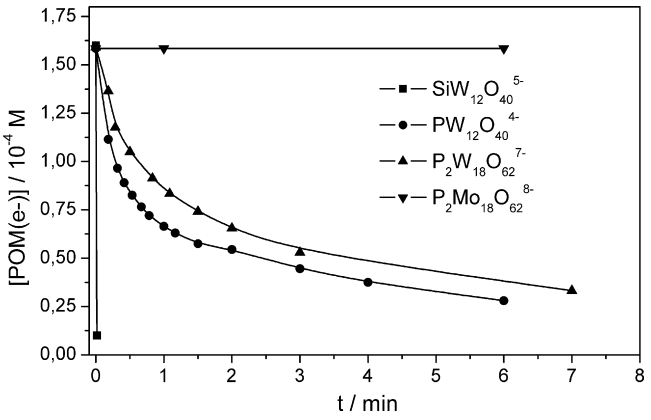

Fig. 8. Thermal (dark) reaction (3): decrease of reduced POM concentration for various POM upon addition of AO 0.05 mM (initial concentration after mixing) in the absence of light.

3.1.6. Thermal reduction of AO by reduced POM

Solutions of blue colored, 1 equiv. reduced tungstates, $PW_{12}O_{40}^{4-}$, $SiW_{12}O_{40}^{5-}$, $P_2W_{18}O_{62}^{7-}$ or 2 equiv. reduced molybdate, $P_2Mo_{18}O_{62}^{8-}$, were produced after photolysis of deaerated aqueous solutions of propan-2-ol 0.5 M, POM 0.25 mM, $HClO_4$ 0.1 M. Photolysis time was adjusted in order to produce the same quantity of reduced POM (ca. 1.5×10^{-4} M) in each POM experiment. After cutting off the light, the photolyzed solutions were mixed with a deaerated solution of AO. The process was monitored at ca. 750 nm, characteristic absorbance of the 1 equiv. reduced tungstates. Upon mixing, a sudden decrease of the absorbance was observed within a few minutes timeframe, indicating that the one-electron reduced tungstates are efficiently reoxidized by dye molecules in the absence of light. Fig. 8 demonstrates the lowering of the concentration of various reduced POM upon the addition of AO. Upon reaction of AO with $SiW_{12}O_{40}^{5-}$ a sudden disappearance of the blue color is noticed within less than 1 s. The process is slower for $PW_{12}O_{40}^{4-}$ and even more for $P_2W_{18}O_{62}^{7-}$, while no reaction takes place in the presence of $P_2Mo_{18}O_{62}^{8-}$. That is, the rate of reduced POM reoxidation by AO follows the order:

$$SiW_{12}O_{40}^{5-} > PW_{12}O_{40}^{4-} > P_2W_{18}O_{62}^{7-} > P_2Mo_{18}O_{62}^{8-} = 0$$

What is more, in all cases, the ratio of the reacted tungstates vs. the reacted AO was found to be ca. 4.

Fig. 9 depicts the function of the initial rate of reoxidation of the 1 equiv. reduced POM, $PW_{12}O_{40}^{4-}$, with the concentration of AO, under equal initial concentration of $PW_{12}O_{40}^{4-}$ (1.3×10^{-4} M). A first-order dependence for AO is noticed:

$$R_0 = k[\mathrm{POM}(e^-)][\mathrm{AO}]$$

and the derived second-order rate constant k ($PW_{12}O_{40}^{4-}$/AO) is 469 M^{-1} s^{-1}.

pH has a detrimental effect in these experiments. Increase of pH from 1 to 4, leads to a great retardation in the rate of reoxidation of $SiW_{12}O_{40}^{5-}$ by AO, reaction (3), increasing the reaction timeframe from less than 1 s to more than 10 min.

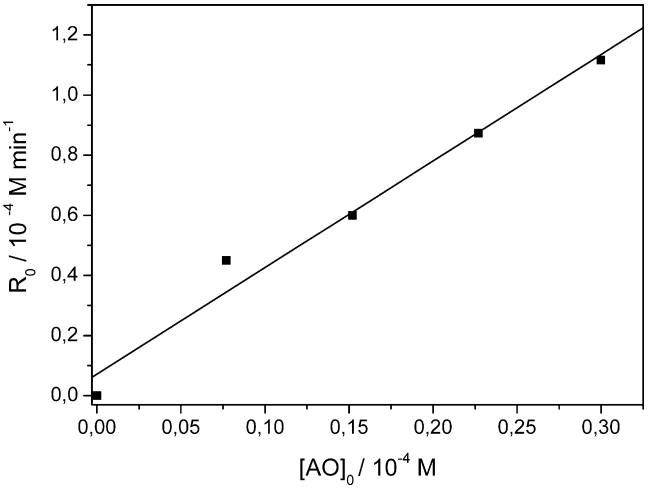

Fig. 9. Thermal (dark) reaction (3): AO first-order dependence of the reoxidation of the 1 equiv. reduced 12-tungstophosphate, $PW_{12}O_{40}^{4-}$, in the absence of light. Deaerated solution containing $PW_{12}O_{40}^{4-}$ 0.13 mM, propan-2-ol 0.5 M (pH 1).

3.2. Photocatalytic oxidative decomposition of AO

An oxygenated solution of AO 0.07 mM, in the presence of $PW_{12}O_{40}^{3-}$ 0.7 mM, illuminated with UV–near vis light, $\lambda > 320$ nm, undergoes gradual decoloration as shown in Fig. 10.

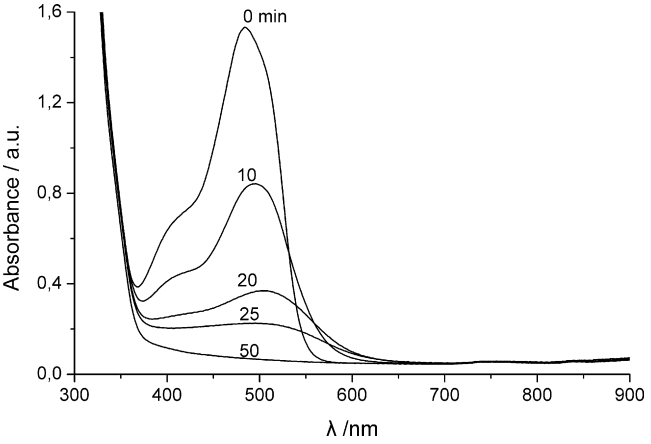

Fig. 10. Oxidative decomposition: variation of spectra of an oxygenated aqueous solution of AO with illumination time. AO 0.07 mM, $H_3PW_{12}O_{40}$ 0.7 mM, $\lambda > 320$ nm. Illumination time is indicated on spectra.

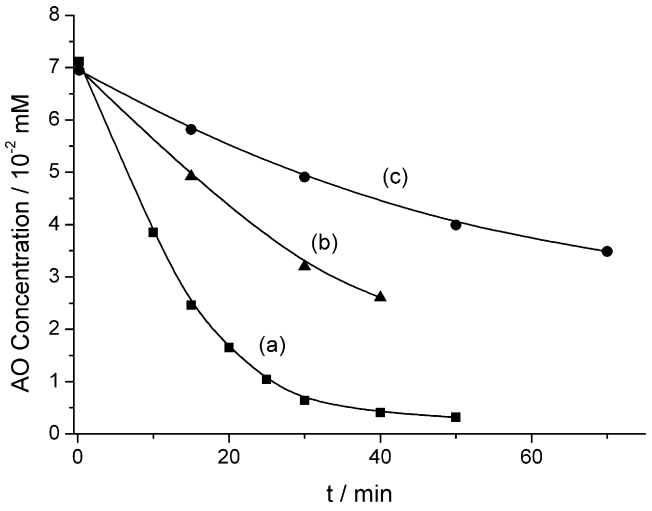

Fig. 11. Oxidative decomposition: decoloration of an oxygenated solution of AO 0.07 mM with illumination time: (a) $H_3PW_{12}O_{40}$ 0.7 mM, pH 1; (b) $H_4SiW_{12}O_{40}$ 0.7 mM, pH 1; (c) $H_4SiW_{12}O_{40}$ 0.7 mM, pH 5. $\lambda > 320$ nm.

3.2.1. The influence of various POM

The influence of two POM ($PW_{12}O_{40}^{3-}$ and $SiW_{12}O_{40}^{4-}$) on the rate of oxidative decoloration of AO has been investigated under similar experimental conditions. The results are shown in Fig. 11.

3.2.2. Identification of intermediates

As mentioned earlier, larger quantities were used for identification of intermediates. Oxygenated (30 ml) aqueous solutions ($PW_{12}O_{40}^{3-}$ 10 mM, AO 1 mM) are photolyzed for different times with UV–near vis light ($\lambda > 320$ nm) under constant stirring and analyzed for intermediates by GC/MS. The characteristic formation and decay of some of the intermediates involved in the process is shown in Fig. 12.

3.2.3. Mineralization of AO

The % decomposition of AO and the concomitant evolution of CO_2 are shown in Fig. 13.

4. Discussion

4.1. Photocatalytic reductive decoloration of AO

The mechanistic scheme suggested to take place during the photocatalytic reductive decoloration of azo dyes in the presence of POM, can be summarized as follows:

$$\mathrm{POM} \overset{h\nu}{\rightleftharpoons} \mathrm{POM}^{*} \quad (1)$$

$$\mathrm{POM}* + \text{propan-2-ol} \rightarrow \mathrm{POM}(e^-) + \text{oxidized products (i.e., } Me_2COH) \quad (2)$$

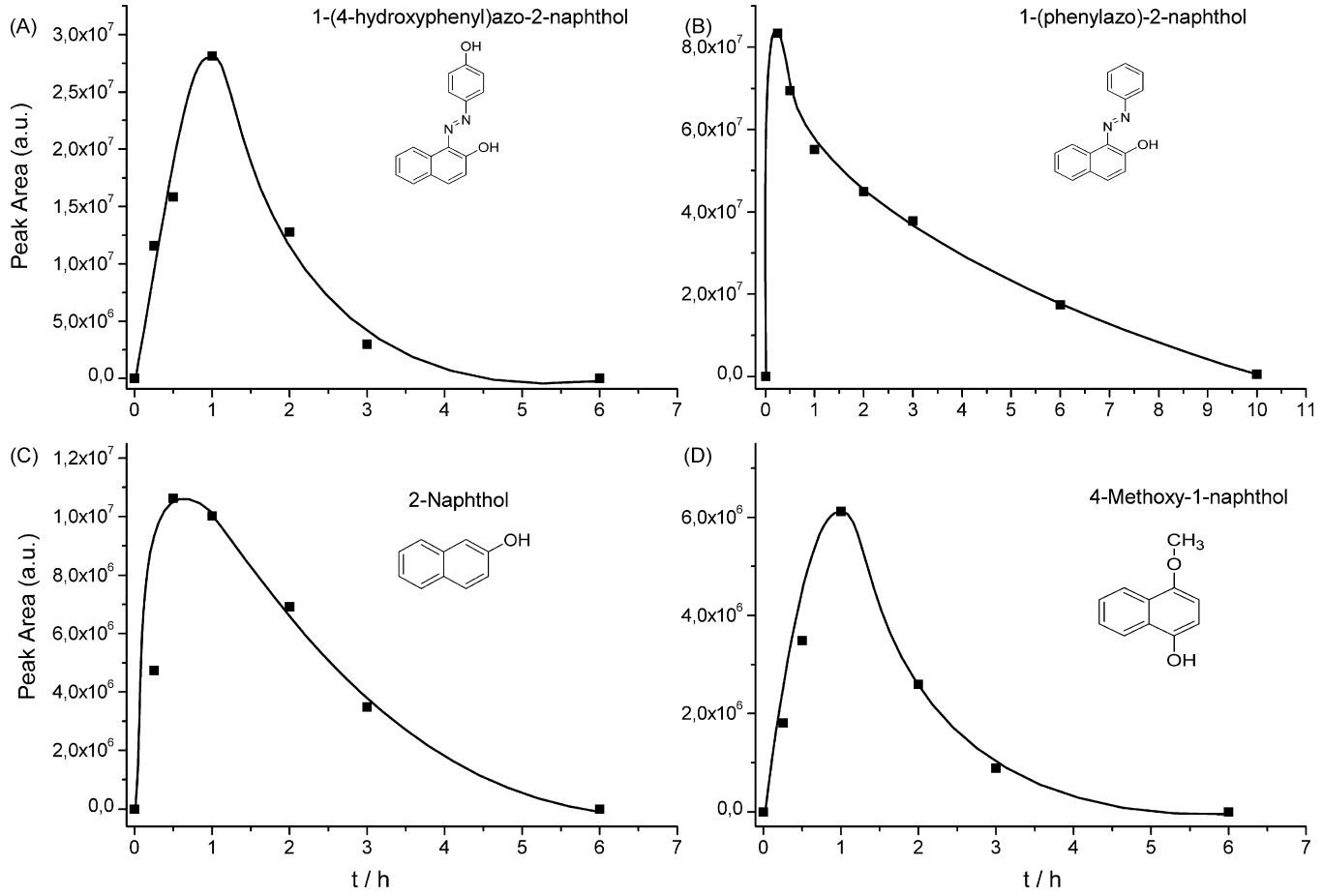

Fig. 12. Characteristic formation and decay of some intermediates involved in the photooxidative decomposition of AO, resulting from a photolyzed ($\lambda > 320$ nm) oxygenated aqueous 30 ml solution of AO (1 mM) containing POM catalyst ($PW_{12}O_{40}^{3-}$, 10 mM).

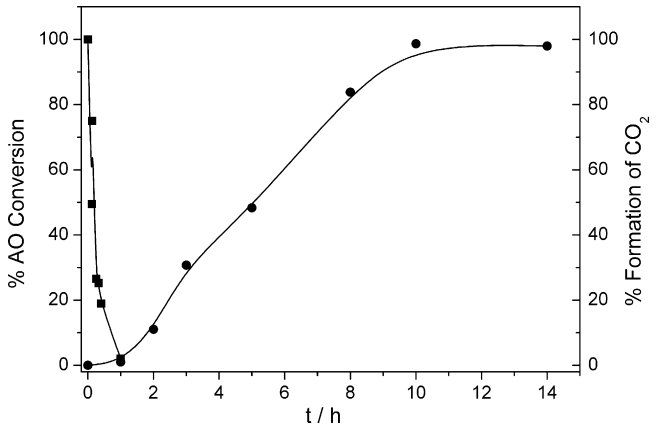

Fig. 13. Oxidative decomposition: % decomposition of AO and % CO_2 evolution, upon illumination of an oxygenated aqueous solution, 4 ml, of AO 0.05 mM, in the presence of $PW_{12}O_{40}^{3-}$ (1 mM) in "illumination box".

$$POM(e^-) + AO \rightarrow POM + \text{reduction products} \quad (3)$$

Reactions (1) and (2) describe the overall photocatalytic oxidation of propan-2-ol and the simultaneous formation of reduced POM. Details, i.e., formation of radicals involved in the process, etc., have been reported elsewhere [11,28–30]. In the presence of the azo dyes molecules, a fast reoxidation of the reduced catalyst occurs (reaction (3)). Thus, no coloration of the solution (in the case of AO with $SiW_{12}O_{40}^{4-}$) or slight coloration (in the case of AO with $PW_{12}O_{40}^{3-}$ and $P_2W_{18}O_{62}^{6-}$) due to blue color of the 1 equiv. reduced tungstates is observed. When the solution is depleted of the dye, the blue colored POM is freely developed. Thermal (dark) independent experiments suggest the ability of reduced POM to reduce efficiently the dye molecules (reaction (3)). There are, however, various ways to inject electrons in POM, for instance: photolysis via a sacrificial reagent, as in this case, electrolysis, reducing reagents, etc. Therefore, dye decoloration, being a thermal process, as mentioned (reaction (3)) is independent of how reduced POM are made.

However, interestingly to note, the decomposition of the dye could also be triggered reductively by the Me_2COH radicals through reaction (4). Pulse radiolysis studies indicate fast reduction of several azo dyes by 2-hydroxy-2-propyl radical with a rate constant of the order of ca. $10^9\ M^{-1}\ s^{-1}$ [31].

$$Me_2COH + AO \rightarrow Me_2CO + \text{reduction products} \quad (4)$$

The lowering of the absorption peaks at 484 nm for AO, characteristic of the –N=N– bond (hydrazone form [32]), is attributed to the break of the azo-bond. The reductive cleavage of the azo-bond in the case of AO dye, requires four electrons and four H^+ in order to be completely reduced, resulting in the formation of sulfanilic acid and 1-amino-2-naphthol (Scheme 2). A 4:1 stoichiometry of reaction (3) for (reduced POM:AO) has been verified in the thermal experiments in accordance with the fact that reduced tungstates are one-electron donors.

Sulfanilic acid was detected as the major degradation product that parallels the degradation of AO, in accordance with the proposed mechanism (Scheme 2). 1-Amino-2-naphthol, the second fraction of the cleavage of the azo-bond was not examined due to the rapid autooxidation reactions of *o*-aminohydroxynaphthalenes [33]. In alliance with the mechanism in Scheme 2, the degradation of AO is highly favored in acidic solutions. We present below how various parameters influence the efficiency of the reductive decoloration of AO.

4.1.1. Propan-2-ol effect

Increasing propan-2-ol concentration favors reaction (2) and subsequently reaction (3) resulting in enhancement of the degradation rate of AO. Thus the whole process is driven by the reductive pathway [21], which results in the selective break of the azo-bond.

In the absence of propan-2-ol the process is still effective (Fig. 5 at zero concentration of propan-2-ol) although much slower and a completely different mechanism is observed; see below.

4.1.2. Dye effect

Increase in dye concentration till an optimum value leads to an increase in the degradation rate, through favoring reactions (3) and (4). Further increase in dye concentration decreases the degradation rate (Fig. 6). This could be attributed to an inner filter effect where dye molecules start absorbing light from the region of POM absorption, as has also been stated before [22].

When $\lambda > 395$ nm is used in order to minimize POM absorption, the degradation of AO is 30 times slower, suggesting that this is not a dye-sensitized process.

4.1.3. Effect of catalyst redox properties: thermodynamic and kinetic effect

The overall efficiency of dye decoloration is kinetically controlled, relating to the rate of formation of reduced catalyst (reaction (2)) following the order $PW_{12}O_{40}^{3-} > SiW_{12}O_{40}^{4-} > P_2W_{18}O_{62}^{6-}$ [34], despite the fact that the thermodynamically controlled thermal reaction (3), between reduced POM and AO, follows a different order, namely, $SiW_{12}O_{40}^{5-} > PW_{12}O_{40}^{4-} > P_2W_{18}O_{62}^{7-}$; see below.

As a matter of comparison, the quantum yields (q.y.) of formation of the 1 equiv. reduced POM at 252 nm has been reported to be ca. 12% for $PW_{12}O_{40}^{4-}$ and 9% for $SiW_{12}O_{40}^{5-}$ [9]. The quantum yield is independent of wavelength below ca. 350 nm [34,35]. Thermal experiments have shown that the stoichiometry of reaction (3) is (4 mol POM)/(1 mol AO). Therefore, the quantum yield of AO decomposition would be four times less, i.e., ~3% when $PW_{12}O_{40}^{3-}$ and ~2.2% in the case of $SiW_{12}O_{40}^{4-}$. These values are close to the value reported for TiO_2 (4.7%) [6], confirming once again the similar efficiency and mechanism of these two processes [11].

Fig. 4 shows the influence of POM concentration in the photodegradation rate of AO. The rate increases, as is always the case, to a plateau above 0.7 mM of POM due to photon saturation (reaction (1)).

Next, the role of redox potentials of POM has been studied independently for thermal reaction (3). The redox potentials are

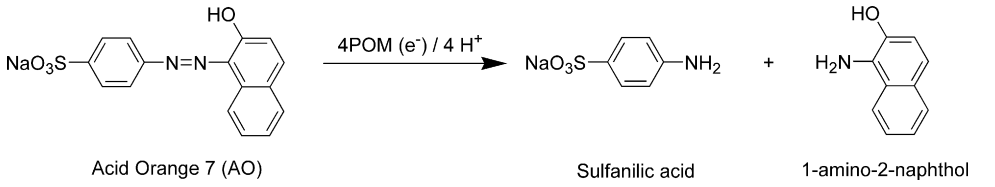

Scheme 2. Mechanism of photocatalytic reductive degradation of AO in the presence of POM.

0.057, 0.221, 0.344 and 0.664 V vs. NHE for $SiW_{12}O_{40}^{4-/5-}$, $PW_{12}O_{40}^{3-/4-}$, $P_2W_{18}O_{62}^{6-/7-}$ and $P_2Mo_{18}O_{62}^{6-/8-}$, respectively, Scheme 1, whereas, the redox potential of AO is 0.76 V vs. NHE [36], making reaction (3) thermodynamically feasible.

Thus, in a two-pot system, a deaerated POM/propan-2-ol solution is illuminated for appropriate time in order to obtain the same concentration of reduced POM, as has already been stated in Section 3.1.6. In turn, the reduced POM, of the same concentration react with AO (reaction (3)). It turns out that the rates follow thermodynamics, that is, the greater the potential difference between reduced POM and AO (Scheme 1) the faster the redox reaction (3). Reduced TiO_2 follows the same rule so that the trend for reaction (3) is

$$TiO_2(e^-) > SiW_{12}O_{40}^{5-} > PW_{12}O_{40}^{4-} > P_2W_{18}O_{62}^{7-} > P_2Mo_{18}O_{62}^{8-}$$

A diffusion-limited reaction between AO and trapped electrons in TiO_2 is reported in the literature, $8.6 \times 10^8\ M^{-1}\ s^{-1}$ [6], greater than those for POM anions, in accordance with the more negative reduction potential of TiO_2. For $SiW_{12}O_{40}^{5-}$, a k value $>2 \times 10^4\ M^{-1}\ s^{-1}$ can be estimated by our data in Fig. 8, according to which the reaction takes place in less than 1 s. This value is consistent with the corresponding rate constant reported by Arslan-Alaton and Ferry, k $(AO/SiW_{12}O_{40}^{5-}) \sim 5.2 \times 10^4\ M^{-1}\ s^{-1}$, derived by competition kinetics [21]. These results, combined with ours concerning the k values, are summarized in Fig. 14. A linear dependence of $\log k$ as a function of the reduction potential is observed for various POM anions and TiO_2 as well, suggesting an outer sphere electron transfer mechanism [23].

4.1.4. Effect of electron scavengers

The introduction of electron acceptors acts in competition with AO. Thermodynamics appears to be the main parameter of the process. For instance, nickel ions do not influence the photodegradation of AO (Fig. 7, curve b) in accordance with the reduction potentials [$E^0(Ni^{2+}/Ni^0) = -0.25$ V vs. NHE and $E^0(PW_{12}O_{40}^{3-/4-}) = 0.221$ V vs. NHE, Scheme 1]. On the contrary, an inhibition in AO decoloration is observed when copper or silver ions are added (Fig. 7, curves c and d). These ions are efficient oxidants for reduced POM [19,20], their efficiency increasing with reduction potential ($Ag^+ > Cu^{2+}$, Scheme 1) and antagonize the reduction of AO. Addition of oxygen (Fig. 7, curve e) causes also a delay in the degradation of the dye. However dioxygen, although it is an effective electron scavenger [14], does not retard the photodecomposition of AO as effectively as Ag^+ (reaction (3)). This could be attributed to the O_2^- and HO_2 radicals formed that are well-known reducing/oxidizing species that could further contribute to the degradation of the azo dye [37].

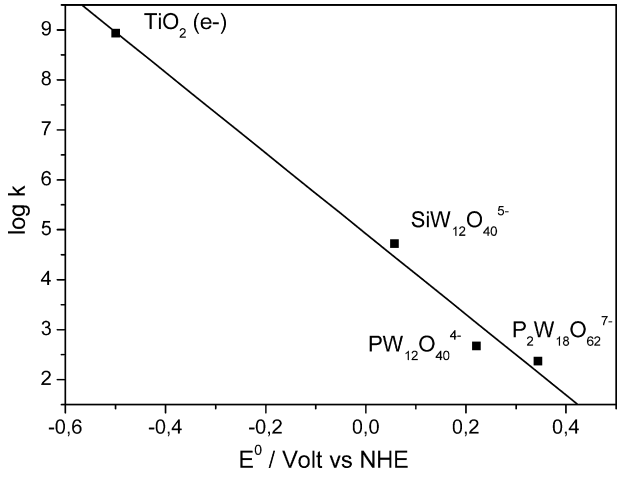

Fig. 14. Thermal (dark) reaction (3): linear function of $\log k$ vs. the reduction potential of various reduced POM and $TiO_2(e^-)$.

4.2. Photocatalytic oxidation of AO

Limited work has shown that AO undergoes photooxidative decomposition by POM, as mentioned earlier, which is true for practically all organic compounds [11] (Figs. 10 and 11). The process involves excitation of POM by UV–near vis light, thereby creating a powerful redox species which, either directly or via OH radicals-mediated reactions, causes mineralization of AO (Fig. 13):

$$POM \overset{h\nu}{\rightleftharpoons} POM^* \quad (1)$$

$$POM* + H_2O \rightarrow POM(e) + OH + H^+ \quad (5)$$

$$POM* + AO \rightarrow POM(e) + (\text{oxidation products}) \quad (6)$$

$$OH + AO \rightarrow OH^- + (\text{oxidation products}) \quad (7)$$

$$\text{Also } POM(e^-) + AO \rightarrow POM + \text{reduction products} \quad (3)$$

This is in analogy to TiO_2 [38] showing once again the overall similarities of photocatalytic processes between TiO_2 and POM [11].

The photodecomposition process goes through several intermediates shown in Scheme 3 prior to evolution of CO_2. The typical formation and decay of some of them is shown in Fig. 12. It turns out, without getting into details, that the oxidative decomposition proceeds with desulfurization of the molecule (intermediate 2) followed by several other intermediates resulting from the replacement of sulfate group by OH (intermediate 1) and breaking of the molecule into naphthalenic (for instance, intermediates 3, 4, 8) and benzoic (intermediate 5) derivatives. It is interesting to note that (intermediate 6) has been detected in the photodecomposition of AO in the presence of all forms of TiO_2 as well as sonication [38]. Another point to consider is the detection of the highly dangerous (intermediate 7). However, as has been pointed out, the overall photocatalytic decomposition of AO in the presence of $PW_{12}O_{40}^{3-}$ results in complete mineralization of the dye.

Fig. 5 shows that the $PW_{12}O_{40}^{3-}$ assisted photoreductive elimination of AO (i.e., in the presence of propan-2-ol) can be more than an order of magnitude faster than the photooxidative one (Fig. 5, the rate at zero concentration of propan-2-ol). Thus the photooxidative process is more effective in that it causes complete mineralization of AO as opposed to reductive decomposition that stops after breaking the (N=N) bond.

4.3. Dye-sensitized decomposition of AO

This process involves absorption of visible light by the dye, followed by charge injection into the catalyst, thus contributing to oxidative decomposition of the dye.

Dye-sensitized TiO_2-assisted degradation has been observed for AO [39–41] and other azo dyes [42,43]. No dye-sensitized POM-assisted degradation of AO has been observed. However, there have been reports on dye-sensitized decomposition of azo dyes by POM in cases where there exists a preassociation of POM with dye, i.e. (a) with dyes bearing positive charge, thereby attracted to negatively charged POM [44] and (b) with POM immobilized in various supports in which the microenvironment supports preassociation of POM with the dyes [45].

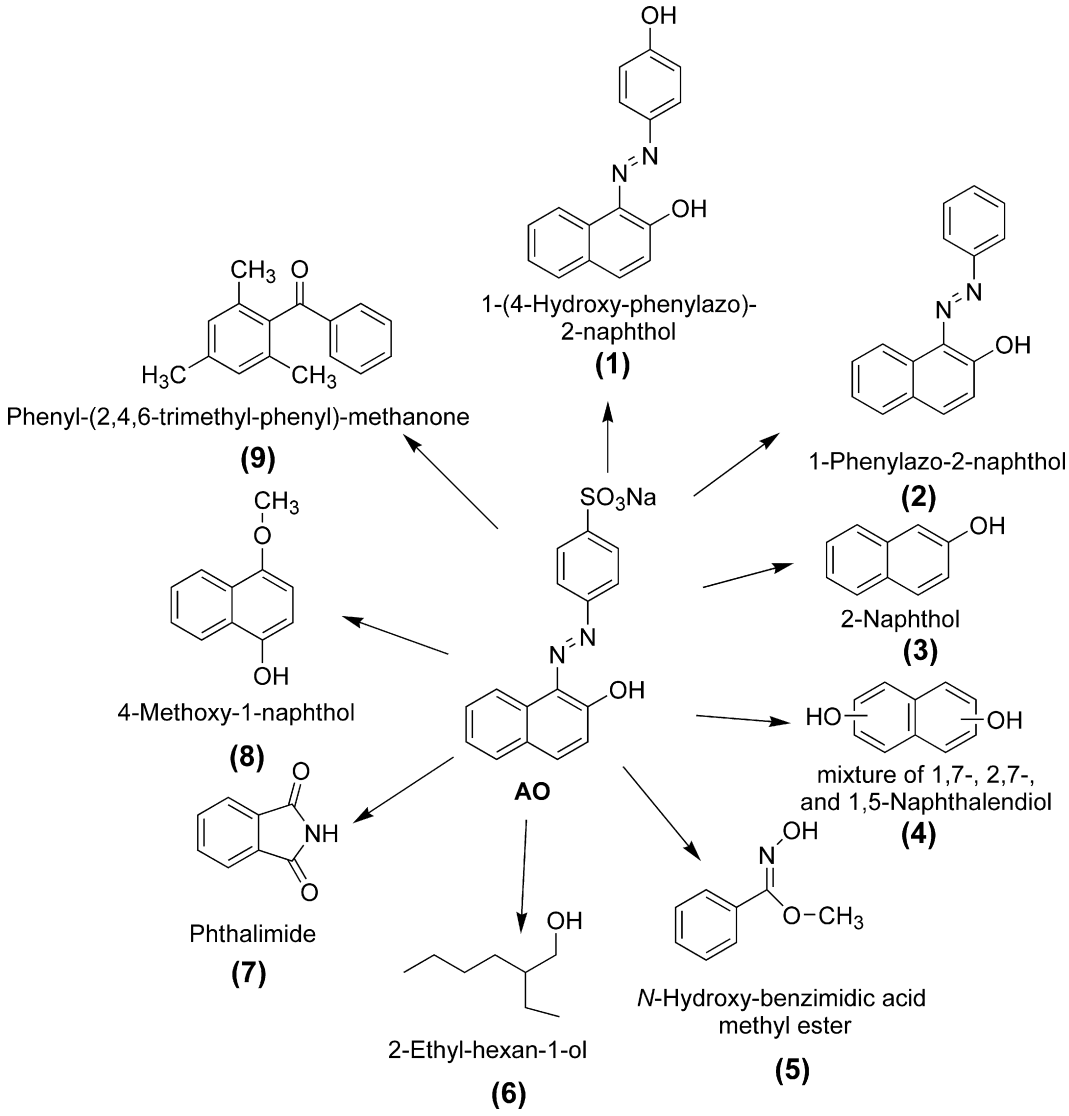

Scheme 3. Photocatalytic oxidative degradation intermediates of AO identified by GC/MS in the presence of $PW_{12}O_{40}^{3-}$.

4.4. Environmental aspect of the process: drawbacks and perspectives

According to the results of this paper, the photoreductive process is effective in a wide range of dye concentration, varying from 5×10^{-7} to more than 10^{-4} M. What is more, prolonged irradiation leads to complete removal of the dye up to non-detected traces (less than 5.0×10^{-7} M). This, in principle, is of great practical advantage compared with heterogeneous processes such as the iron-based treatment, which cannot be quantitative, leaving ca. 4% of the target azo dye unaffected [46].

However, toxic amines are released upon reduction of the azo dye. This has made European Union (then EEC) to proceed to regulations concerning marketing of dyes that are capable of reductively releasing carcinogenic amines [47]. Thus, the products of reductive treatment are not environmentally friendlier. However, the slower oxidative decomposition leads to mineralization of AO.

Acknowledgments

We thank P.V. Kamat and the Radiation Laboratory, University of Notre Dame, USA for helpful discussions, for their hospitality and support. We thank the Ministry of Development, General Secretariat of Research and Technology of Greece for supporting part of this work in the frame of a USA-Greece exchange project. A.T. and T.T are grateful to NCSR Demokritos, Institute of Physical Chemistry, for postdoctoral fellowships.

References

[1] M.S. Reisch, Chem. Eng. News 66 (1988) 7–14.
[2] R. Jain, M. Bhargava, N. Sharma, J. Sci. Ind. Res. India 62 (2003) 813–819.
[3] F.P. van der Zee, G. Lettinga, J.A. Field, Water Sci. Technol. 42 (2000) 301–308.
[4] J.S. Cao, L.P. Wei, Q.G. Huang, L.S. Wang, S.K. Han, Chemosphere 38 (1999) 565–571.
[5] J.R. Perey, P.C. Chiu, C.P. Huang, D.K. Cha, Water Environ. Res. 74 (2002) 221–225.
[6] K. Vinodgopal, I. Bedja, S. Hotchandani, P.V. Kamat, Langmuir 10 (1994) 1767–1771.
[7] K. Vinodgopal, P.V. Kamat, J. Photochem. Photobiol. A: Chem. 83 (1994) 141–146.
[8] C. Nasr, K. Vinodgopal, S. Hotchandani, A.K. Chattopadhyay, P.V. Kamat, Res. Chem. Intermed. 23 (1997) 219–231.
[9] E. Papaconstantinou, Chem. Soc. Rev. 16 (1989) 1–31, and references therein.
[10] T. Yamase, Catal. Surv. Asia 7 (2003) 203–217.
[11] A. Hiskia, A. Mylonas, E. Papaconstantinou, Chem. Soc. Rev. 30 (2001) 62–69, and references therein..
[12] A. Mylonas, E. Papaconstantinou, J. Mol. Catal. 92 (1994) 261–267.
[13] E. Androulaki, A. Hiskia, D. Dimotikali, C. Minero, P. Calza, E. Pelizzetti, E. Papaconstantinou, Environ. Sci. Technol. 34 (2000) 2024–2028.
[14] A. Hiskia, E. Papaconstantinou, Inorg. Chem. 31 (1992) 163–167.
[15] A. Ioannidis, E. Papaconstantinou, Inorg. Chem. 24 (1985) 439–441.

[16] R. Amadelli, G. Varani, A. Maldotti, V. Carassiti, J. Mol. Catal. 59 (1990) L9–L14.
[17] A. Troupis, A. Hiskia, E. Papaconstantinou, New J. Chem. 25 (2001) 361–363.
[18] A. Troupis, A. Hiskia, E. Papaconstantinou, Angew. Chem. Int. Ed. 41 (2002) 1911–1914.
[19] A. Troupis, A. Hiskia, E. Papaconstantinou, Environ. Sci. Technol. 36 (2002) 5355–5362.
[20] A. Troupis, A. Hiskia, E. Papaconstantinou, Appl. Catal. B: Environ. 42 (2003) 305–315.
[21] I. Arslan-Alaton, J.L. Ferry, J. Photochem. Photobiol. A: Chem. 152 (2002) 175–181.
[22] I. Arslan-Alaton, Dyes Pigments 60 (2004) 167–176.
[23] I.A. Weinstock, Chem. Rev. 98 (1998) 113–170.
[24] A. Troupis, E. Gkika, T. Triantis, A. Hiskia, E. Papaconstantinou, J. Photochem. Photobiol. A: Chem. 188 (2007) 272–278.
[25] M.T. Pope, G.M. Varga, Inorg. Chem. 5 (1966) 1249–1254.
[26] M.T. Pope, Heteropoly and Isopoly Oxometalates: Inorganic Chemistry Concepts (Inorganic Chemistry Concepts, vol. 8), Springer–Verlag, Berlin, 1983.
[27] G.M. Varga, E. Papaconstantinou, M.T. Pope, Inorg. Chem. 9 (1970) 662–667.
[28] A. Mylonas, A. Hiskia, E. Androulaki, D. Dimotikali, E. Papaconstantinou, Phys. Chem. Chem. Phys. 1 (1999) 437–440.
[29] P. Kormali, T. Triantis, D. Dimotikali, A. Hiskia, E. Papaconstantinou, Appl. Catal. B: Environ. 68 (2006) 139–146.
[30] T. Yamase, T. Kurozumi, J. Chem. Soc., Dalton Trans. 10 (1983) 2205–2209.
[31] K.K. Sharma, P. O'Neill, J. Oakes, S.N. Batchelor, B.S.M. Rao, J. Phys. Chem. A 107 (2003) 7619–7628.
[32] M. Stylidi, D.I. Kondarides, X.E. Verykios, Appl. Catal. B: Environ. 40 (2003) 271–286.
[33] M. Kudlich, M.J. Hetheridge, H.J. Knackmuss, A. Stolz, Environ. Sci. Technol. 33 (1999) 896–901.
[34] D. Dimoticali, E. Papaconstantinou, Inorg. Chim. Acta 87 (1984) 177–180.
[35] R.R. Ozer, J.L. Ferry, J. Phys. Chem. 106 (2002) 4336–4342.
[36] K. Vinodgopal, P.V. Kamat, Environ. Sci. Technol. 29 (1995) 841–845.
[37] C.C. Chen, X.Z. Li, W.H. Ma, J.C. Zhao, H. Hidaka, N. Serpone, J. Phys. Chem. 106 (2002) 318–324.
[38] T. Velegraki, I. Poulios, M. Chalarabaki, N. Kalogerakis, P. Samaras, D. Mantzavinos, Appl. Catal. B: Environ. 62 (2006) 159–168.
[39] K. Vinodgopal, D.E. Wynkoop, P.V. Kamat, Environ. Sci. Technol. 30 (1996) 1660–1666.
[40] M. Stylidi, D.I. Kondarides, X.E. Verykios, Appl. Catal. B: Environ. 47 (2004) 189–201.
[41] M. Stylidi, D.I. Kondarides, X.E. Verykios, Int. J. Photoenergy 5 (2003) 59–67.
[42] J.C. Zhao, C.C. Chen, W.H. Ma, Top. Catal. 35 (2005) 269–278.
[43] I. Konstantinou, T. Albanis, Appl. Catal. B: Environ. 49 (2004) 1–14.
[44] C.C. Chen, W. Zhao, P. Lei, J. Zhao, N. Serpone, Chem. Eur. J. 10 (2004) 1956–1965.
[45] P.X. Lei, C.C. Chen, J. Yang, W.H. Ma, J.C. Zhao, L. Zhang, Environ. Sci. Technol. 39 (2005) 8466–8474.
[46] S. Nam, P.G. Tratnyek, Water Res. 34 (2000) 1837–1845.
[47] European Union Directive No. 76/769/EEC, OJ L 262, September 27, 1976, p. 201.